

Structural, Magnetic, and Conductivity Properties of Charge-Transfer Salts Derived from Metallacarboranes

Yaw-Kai Yan and D. Michael P. Mingos

Chemistry Department, Imperial College of Science, Technology, and Medicine, South Kensington, London SW7 2AY, U.K.

1 Introduction

Low-dimensional ionic molecular solids have been the subject of intense research activity for over two decades because in many cases, they exhibit interesting electrical¹ and magnetic properties.^{2,3} Co-operative magnetic phenomena, for example, have been observed in a series of salts containing $S \geq \frac{1}{2}$ decamethyl-metallocene cations and planar polycyano-organic radical anions.² Miller and co-workers rationalized the magnetic behaviour of these salts using the extended-McConnell configurational admixture model.³ Although this model is useful in explaining and predicting the magnetic properties of most of the known metallocene-based salts, its assumptions and its general validity have been questioned.⁴

In an attempt to further test the extended-McConnell model and to establish a new class of molecular magnetic materials, it was decided to synthesize and study several molecular salts incorporating metallacarborane sandwich complexes of the *nido*-[7,8-C₂⁻H₁₁]²⁻ ligand and their substituted analogues (Figure 1). The chemical behaviour of these complexes has been widely studied by Hawthorne,⁵ but their potential in this area of molecular electronics has not previously been addressed. The metallacarborane complexes have the advantage of being more stable⁶ than their corresponding metallocene analogues, with which they are isoelectronic. The occurrence of the anionic metallacarborane complexes affords the opportunity of studying salts with organic radical cations (*e.g.* those derived from TTF and ET, see Figure 2), which are complementary to the metallocenium salts with anionic organic radicals. The possible formation of charge-transfer salts containing stacked organic donor molecules in mixed oxidation states is also of interest since these salts may show novel conducting properties.¹

2 Discussion

2.1 TTF Salts with Unsubstituted Metallacarborane Anions⁷

The TTF⁺ salts of the unsubstituted metallacarborane anions, [TTF]⁺[M(C₂B₉H₁₁)₂]⁻ [(1), M = Cr; (2), M = Fe; (3), M = Ni] have the metal ions in a formal oxidation state of + 3,

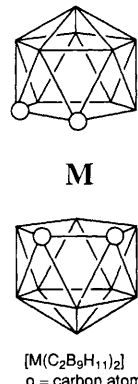


Figure 1 The molecular structure of a typical sandwich complex of the *nido*-[7,8-C₂⁻H₁₁]²⁻ ligand.

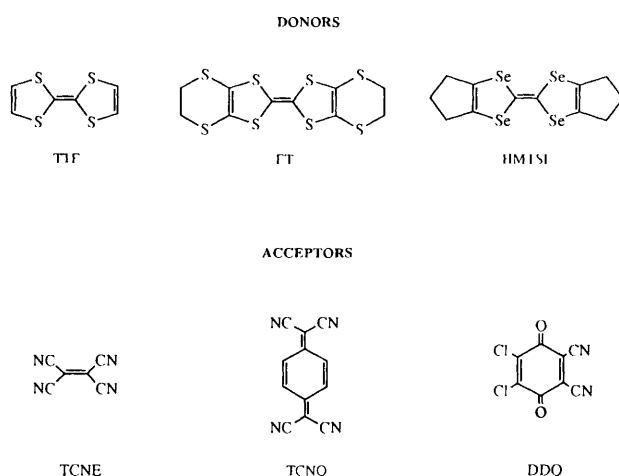
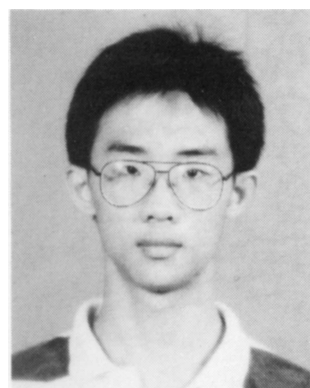


Figure 2 Selected organic donors and acceptors used for the synthesis of molecular materials.

Yaw-Kai Yan was born in Singapore in 1967. He obtained his B.Sc. (Hons.) in 1990 from the National University of Singapore, where he stayed on for M.Sc. research on the chemistry of rhodium carbonyl complexes. In 1991 he began Ph.D. research with Professor Mingos, working on charge-transfer salts based on metallacarborane complexes. He obtained his Ph.D. in February 1995 and joined the academic staff of the Nanyang Technological University, Singapore, in May 1995.



Michael Mingos was born in Basra, Iraq in 1944 and emigrated to England in 1950. He obtained a B.Sc. from UMIST in 1965 and a D.Phil. from Sussex University in 1968. After post-doctoral work with Professor J. A. Ibers and Professor Sir Ronald Mason he took up his first academic appointment at Queen Mary College, University of London. From 1976-92 he was at Oxford University and since 1992 he has held the Sir Edward Frankland B. P. Chair at Imperial College.



but with d^3 , d^5 , and d^7 electronic configurations. The commonly-employed method of preparing TTF^+ salts by metathetical reaction with $[\text{TTF}]_3[\text{BF}_4]_2$ in acetonitrile⁸ proved not to be feasible for the preparation of compounds (1)–(3) as the resulting salts are more soluble in acetonitrile than $[\text{TTF}]_3[\text{BF}_4]_2$. The charge-transfer salts (1) and (2) were prepared in good yields by the metathesis reaction of $[\text{TTF}]^+$ with $\text{Cs}[\text{Cr}(\text{C}_2\text{B}_9\text{H}_{11})_2]$ or $\text{Na}[\text{Fe}(\text{C}_2\text{B}_9\text{H}_{11})_2]$, respectively, in water. The corresponding nickelacarborane charge-transfer salt (3) was obtained as large black crystals by the slow evaporation of a $\text{CH}_2\text{Cl}_2/n\text{-hexane}$ (1:1) solution containing neutral TTF and the Ni^{IV} complex *commo*-[3,3'- $\text{Ni}(\text{C}_2\text{B}_9\text{H}_{11})_2$] in equimolar quantities.

The crystal lattice of (1) consists of chains of alternating $[\text{TTF}]^+$ and $[\text{Cr}(\text{C}_2\text{B}_9\text{H}_{11})_2]^-$ ions which extend in the *c*-direction, as shown in Figure 3. The crystal structure may also be described in terms of alternating layers of $[\text{TTF}]^+$ and $[\text{Cr}(\text{C}_2\text{B}_9\text{H}_{11})_2]^-$ ions. No intermolecular bonding interactions are evident amongst the $[\text{TTF}]^+$ ions, the closest intermolecular $\text{S}\cdots\text{S}$ contact being 3.96 Å. There are also no short cation–anion or anion–anion contacts. The shortest intrachain $\text{Cr}\cdots\text{S}$ distances are 5.93 and 5.94 Å and the shortest interchain $\text{Cr}\cdots\text{S}$ distances are 6.75 and 6.76 Å.

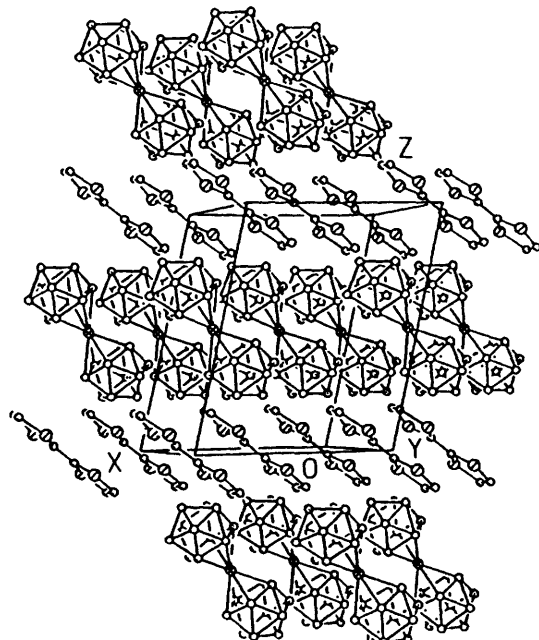


Figure 3 Stereoscopic view of the packing of ions in crystals of (1).

In contrast to (1), discrete stacked dimers of $[\text{TTF}]^+$ cations occur in the crystal structures of (2) and (3), which are isomorphous, as shown in Figure 4. The $[\text{TTF}]^+$ cations within the dimers are centrosymmetrically related and are fully eclipsed, with an interplanar separation of 3.44 Å. Short intradimer $\text{S}\cdots\text{S}$ contacts of *ca.* 3.4 Å indicate significant bonding interactions between the paired $[\text{TTF}]^+$ ions making up the dimers.

It is noteworthy that the molecular packing observed in (2) and (3) differs drastically from that observed in (1). An attempt to grow crystals of (2) which are isomorphous to (1) by seeding an acetone–ethanol solution of (2) with microcrystals of (1) was unsuccessful. The significantly lower density of crystals of (1) (1.365 g cm^{–3}) compared to those of (2) (1.426 g cm^{–3}) and (3) (1.437 g cm^{–3}) implies that the molecular packing in (1) is less efficient than that in (2) and (3). In an attempt to understand why the packing in (1) differs from that in (2) and (3), the molecular volumes, V_m , and the moments of inertia, M_1 , M_2 , and M_3 ($M_1 \geq M_2 \geq M_3$) of the metallacarborane anions in (1), (2), and (3) were calculated. The results are tabulated in Table 1. It can be seen that, whilst the molecular volumes of the three anions are very similar, the $[\text{Cr}(\text{C}_2\text{B}_9\text{H}_{11})_2]^-$ anion is significantly more prolate than its iron and nickel analogues. The greater prolateness of the chromacarborane anion is reflected in the lower

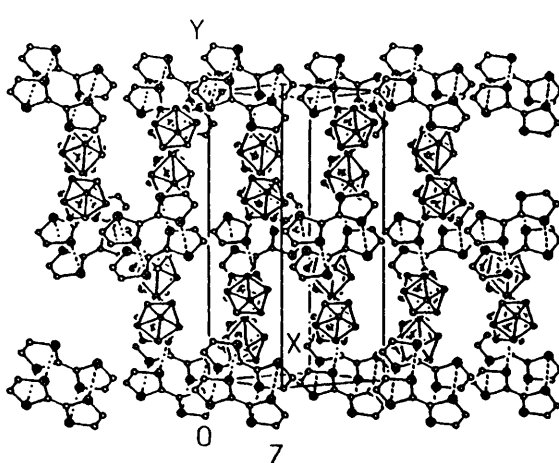
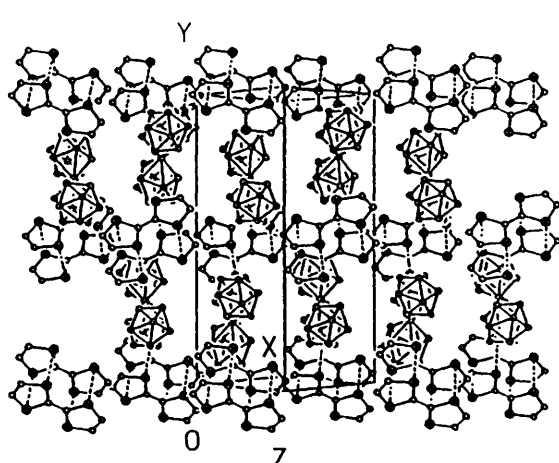
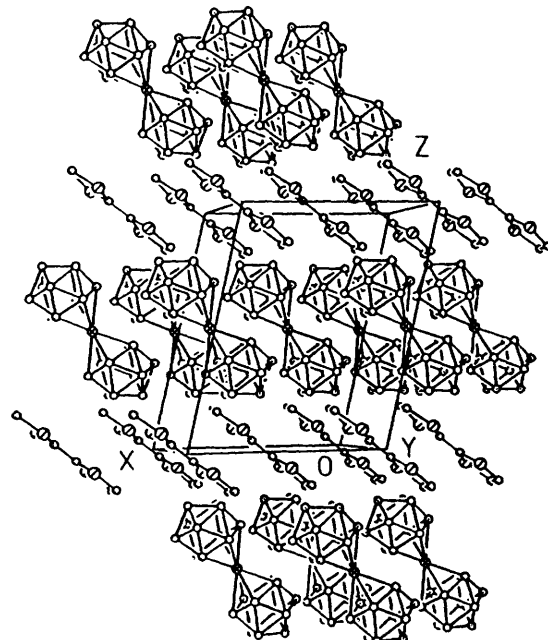


Figure 4 Stereoscopic view of the molecular packing of (2) down the (10–1) direction.

Table 1 Volumes and moments of inertia^a of anions in compounds (1)–(3)

Anion	[Cr(C ₂ B ₉ H ₁₁) ₂]	[Fe(C ₂ B ₉ H ₁₁) ₂]	[Ni(C ₂ B ₉ H ₁₁) ₂]
$V^m/\text{\AA}^3$	277.0	277.2	270.8
$M_1/\text{\AA}^2$	361	327	329
$M_2/\text{\AA}^2$	82	85	82
$M_3/\text{\AA}^2$	80	83	80

^a Moments of inertia were calculated without mass weighting

dimensionality of the molecular packing in (1), in which the anions form sheets rather than the three-dimensional networks observed in (2) and (3).

No cooperative magnetic behaviour is observed in compounds (1)–(3) down to 6 K. The corrected molar magnetic susceptibilities of these compounds follow the Curie–Weiss expression, $\chi = C/(T - \theta)$, with small values of θ (−2.5 K for (1), −2.0 K for (2), and +1.5 K for (3)), indicative of negligible interaction between the unpaired spins of the ions in the solids. Correspondingly, the effective magnetic moments, $\mu_{\text{eff}} = \sqrt{(8\chi T)}$, of all three compounds are effectively independent of temperature. The absence of monomeric [TTF]⁺ radical cations in the crystals of (2) and (3) is reflected in their μ_{eff} values (2.4 and 1.7 μ_B), which are characteristic of the [Fe(C₂B₉H₁₁)₂] and [Ni(C₂B₉H₁₁)₂] anions respectively. The failure to observe cooperative magnetic behaviour in (2) and (3) is consistent with the extended-McConnell model, in which cooperative magnetic behaviour is only possible in systems where both the cation and anion have unpaired spins.³

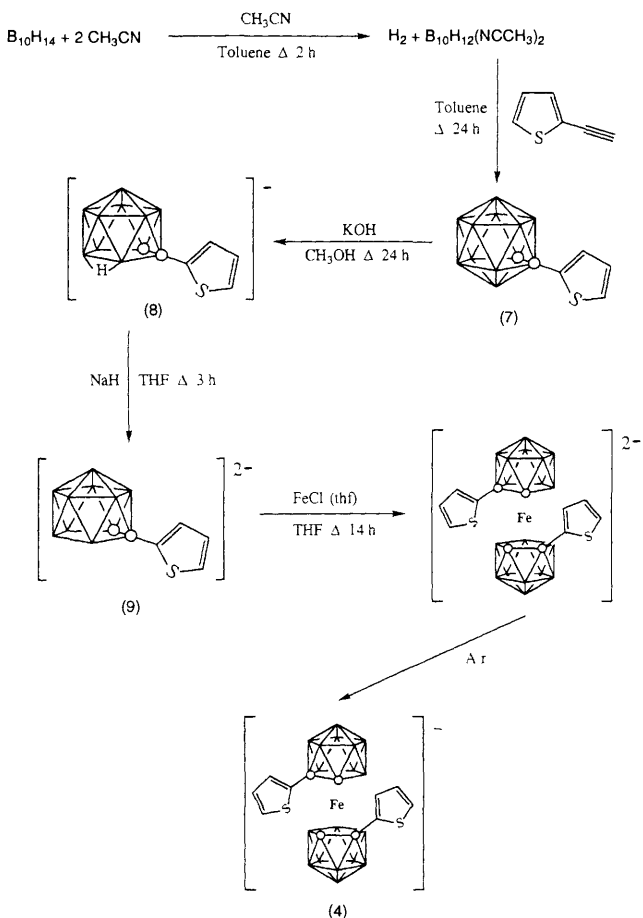
The μ_{eff} of (1), 3.96 μ_B , is slightly lower than the value of 4.22 μ_B calculated using the formula for two non-interacting spins $[(\mu_{\text{eff}})_{\text{total}}]^2 = [(\mu_{\text{eff}})_{\text{cation}}]^2 + [(\mu_{\text{eff}})_{\text{anion}}]^2$, assuming the μ_{eff} values of 1.73 and 3.85 μ_B for the cation and anion respectively. The Cr–S distances of 5.9 and 6.8 Å in (1) (*vide supra*) are comparable to the Fe–N(TCNE) distances of 5.5–6.5 Å in [Cp₂*Fe]⁺[TCNE]⁺ which is a bulk ferromagnet below 5 K ($\theta = +30$ K).² The lack of any significant cooperative behaviour of (1) even at 6 K thus casts doubt on the simple mechanism proposed by Miller and co-workers to explain the spin-coupling between [Cp₂*Fe]⁺ and [TCNE]⁺, since Miller's mechanism involves spin exchange between the Fe atom of [Cp₂*Fe]⁺ and N atoms of [TCNE].²

Conductivity measurements performed on crystals of compounds (1) and (3) indicate that (1) is a semiconductor ($\sigma_{\text{RT}} = 3 \times 10^{-4}$ S cm^{−1}, activation energy = 0.16 eV) and (3) is an insulator ($\sigma_{\text{RT}} \leq 10^{-7}$ S cm^{−1}).⁹ The high resistivity of compound (3) is consistent with the presence of isolated (TTF⁺)₂ dimers in its crystal lattice.

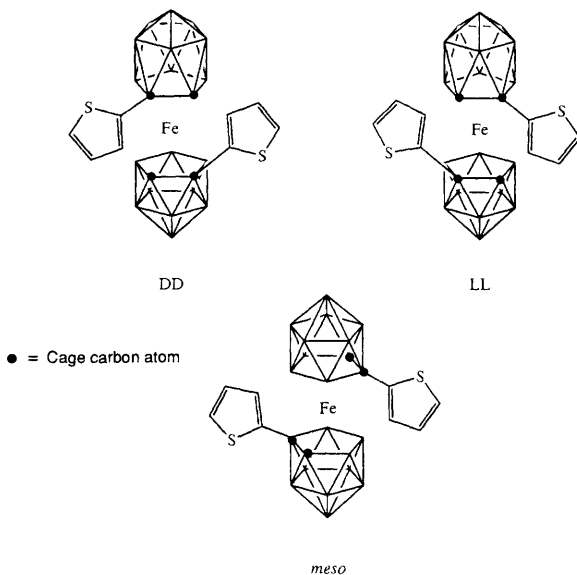
2.2 TTF Salts of a Thiophene-functionalized Ferracarborane Anion⁹

Since intermolecular attractive interactions between sulfur atoms are known to exert a strong influence on the packing of molecules in crystals,¹ it was envisaged that the introduction of thiophene substituents on the metallacarborane anion may enhance the TTF-metallacarborane interaction *via* S–S contacts, thereby suppressing dimerization of TTF units and encouraging the propagation of mixed-valence TTF stacks. Such an arrangement of TTF units is expected to show a higher electrical conductivity.¹ Alternatively, the thiophene groups may also engage in π – π interactions with the TTF units to produce unusual molecular arrangements, such as interleaved mixed stacks which lie in close proximity to the paramagnetic metal centres. This arrangement may favour magnetic interaction between the spins on the cations and anions.

The synthesis of the thiophene-substituted ferracarborane *commo*-[3,3'-Fe{1-(thiophene-2-yl)-1,2-C₂B₉H₁₀}₂][−] (4) is summarized in Scheme 1. Since the asymmetric *nido*-[7-C₄H₃S]-7,8-



Scheme 1 Synthesis of complex (4)

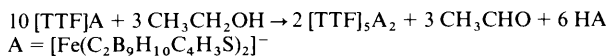


Scheme 2 The stereoisomers of complex (4)

C₂B₉H₁₀^{2−} (9) is expected to be formed as a racemate, complex (4) should be produced as a mixture of *meso* (DL), DD, and LL isomers (see Scheme 2). However, it has so far proved impossible to resolve the isomeric mixture. In fact, there is yet no evidence for the existence of the *meso*-isomer, since only the DD and LL forms were detected in the crystal structures of the TTF salts (5) and (6) (*vide infra*).

Reaction of [TTF]⁺Cl[−] with the sodium salt of complex (4) in

aqueous solution led to the formation of $[\text{TTF}]^+[\text{Fe}(\text{C}_2\text{B}_9\text{H}_{10}\text{C}_4\text{H}_3\text{S})_2]_2^-$ (6). Attempts to grow single crystals of the 1 1 salt from an acetone–ethanol mixture by slow evaporation yielded black plate-like crystals of the 5 2 mixed-valence salt $[\text{TTF}]_5[\text{Fe}(\text{C}_2\text{B}_9\text{H}_{10}\text{C}_4\text{H}_3\text{S})_2]_2$ (5) instead. The most probable source of the neutral/partially-oxidized TTF molecules in (5) is the reduction of $[\text{TTF}]^+$ by ethanol



It is noteworthy, however, that slow evaporation of an acetone–ethanol solution containing $[\text{TTF}]^+[\text{Fe}(\text{C}_2\text{B}_9\text{H}_{11})_2]^-$ and half a molar equivalent of TTF yielded only crystals of $[\text{TTF}]^+[\text{Fe}(\text{C}_2\text{B}_9\text{H}_{11})_2]^-$. This suggests that the $[\text{Fe}(\text{C}_2\text{B}_9\text{H}_{10}\text{C}_4\text{H}_3\text{S})_2]^-$ anion itself favours the selective crystallization of the mixed-valence salt (5).

The formula unit of $[\text{TTF}]_5[\text{Fe}(\text{C}_2\text{B}_9\text{H}_{10}\text{C}_4\text{H}_3\text{S})_2]_2$ (5) contains both DD- and LL- isomers of the $[\text{Fe}(\text{C}_2\text{B}_9\text{H}_{10}\text{C}_4\text{H}_3\text{S})_2]^-$ anion, which are related by a crystallographic inversion centre. The crystal lattice features centrosymmetric stacked trimers of TTF units which propagate along the *a*-axis, as shown in Figure 5. The interplanar separation between the TTF units within a trimer is 3.47 Å, whilst that between adjacent trimers is 3.54 Å. Adjacent TTF trimers are bridged in the *c*-direction by another TTF unit, which lies approximately orthogonally to the TTF units in the trimers. Short S–S contacts of 3.56 Å link the bridging TTF to the centrosymmetrically related TTF trimers on either side, as illustrated in Figure 6. The continuous two-dimensional layer of linked TTF trimers produced is unprecedented, the only other examples of this type of ‘orthogonal’ S–S linkage by TTF units occurs in $[\text{TTF}]_3[\text{Pt}(\text{S}_2\text{C}_2\text{O}_2)_2]$ and $[\text{TTF}]_2[\text{Ni}(\text{S}_2\text{C}_2\text{H}_2)_2]$, where the linkage is between TTF dimers.^{10,11} For the nickel(II) crystal, electrical conductivity along the bridging direction was established, indicating an appreciable interaction between the dimers and the bridging TTF units. A similar packing motif also occurs in the crystal structure of $[\text{HMTTeF}]_4[\text{PF}_6]_2$ (HMTTeF = hexamethylene-tetratellurofulvalene), which adopts a layered structure featuring stacked trimers of HMTTeF units linked *via* short Te–Te contacts with a bridging HMTTeF unit.¹²

The only TTF–thiophene short S–S contacts involve TTF

units which are isolated from the TTF sheets in the crystal (S–S 3.50 Å). Each of these TTF units bridges the thiophene-2-yl groups of two adjacent centrosymmetrically related ferracarborane anions. These TTF-linked anion pairs propagate along the *a*-axis to form a continuous ‘ribbon’. Therefore, the overall structure consists of layers of these ‘ribbons’ alternating with the TTF sheets as illustrated in Figure 5.

Single crystals of toluene-solvated (6) were grown by layering an acetone–dichloromethane (1:1) solution of (6) with toluene at *ca* –20 °C. As in the structure of (5), both the DD- and LL-isomers of the $[\text{Fe}(\text{C}_2\text{B}_9\text{H}_{10}\text{C}_4\text{H}_3\text{S})_2]^-$ anion are present in $[\text{TTF}]^+[\text{Fe}(\text{C}_2\text{B}_9\text{H}_{10}\text{C}_4\text{H}_3\text{S})_2]_2\text{C}_7\text{H}_8$ (6). The $[\text{TTF}]^+$ cations form centrosymmetric stacked dimers in the crystal lattice, as shown in Figure 7. The $[\text{TTF}]^+$ units in each dimer are virtually eclipsed, with an interplanar separation of 3.45 Å, and feature short intradimer S–S distances of 3.4–3.5 Å. Each $[\text{TTF}]^+_2$ dimer is effectively isolated from other dimers by the surrounding anions and toluene solvate molecules. The toluene molecules are oriented in a face-to-edge manner with respect to the $[\text{TTF}]^+$ units, with a relatively short distance of 3.43 Å between S(1b) and the toluene ring centroid. This indicates that there is an electrostatic attraction between the $[\text{TTF}]^+$ cation and the π -electron cloud of the solvate which stabilizes their juxtaposition in the crystal lattice.

Between 25 and 295 K the corrected molar magnetic susceptibilities of compounds (5) and (6) (the toluene-solvated crystals) follow the Curie–Weiss law, with θ values of +1.9 and +0.5 K respectively. The θ values indicate that there is very weak ferromagnetic interaction between the unpaired spins of the ions in both compounds. In accordance with the presence of spin-paired TTF trimers and dimers in compounds (5) and (6) respectively, there is no contribution from the $[\text{TTF}]^+$ cations to the overall susceptibilities of the compounds. The average moment $\mu_{\text{av}} = \sqrt{(8C)}$ of (5) between 25 and 295 K (3.0 μ_{B}) indicates the presence of two low-spin Fe^{III} centres, each having a moment of 2.2 μ_{B} , per formula unit of the compound [$\mu_{\text{total}}^2 = 2\mu_{\text{Fe}^{(\text{III})}}^2$]. The corresponding value for (6) (2.0 μ_{B}) is consistent with the presence of one low-spin Fe^{III} centre per formula unit.

One of the criteria for intermolecular ferromagnetic coupling is that there must be no overlap between the magnetic orbitals of adjacent molecules.¹³ This condition appears to be satisfied in

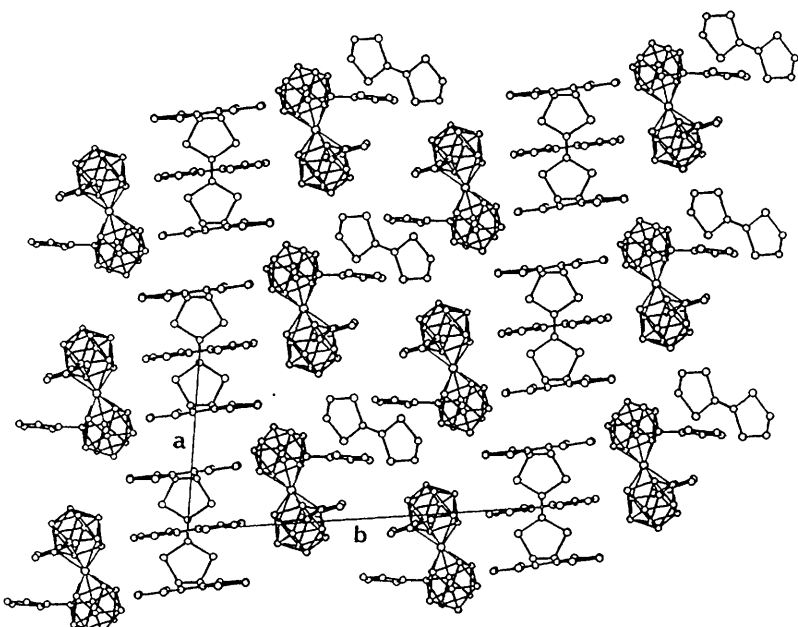


Figure 5 The crystal packing of (5), viewed down the *c*-axis

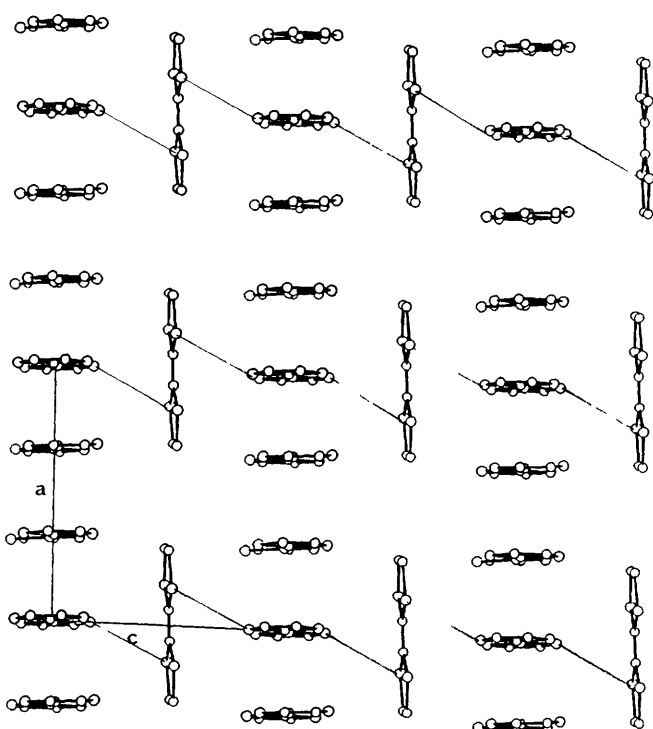


Figure 6 The two-dimensional sheet of interacting TTF units in the crystal lattice of compound (5), viewed down the *b*-axis. The thin lines joining TTF units along the *c* direction indicate the short S-S contacts

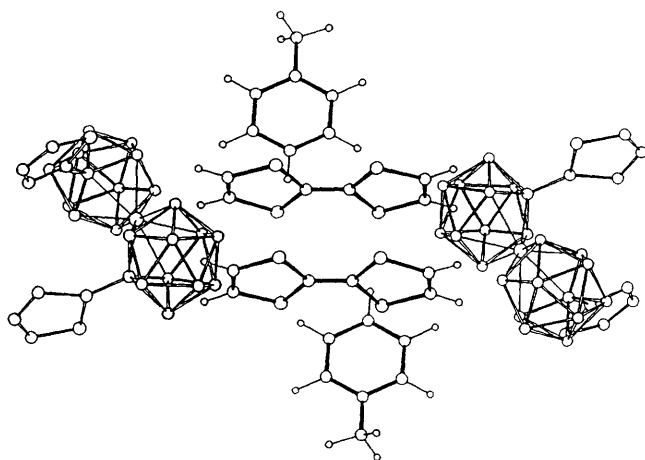


Figure 7 The centrosymmetric unit of compound (6)

both compounds (5) and (6) since there is no short inter-anion contact in either compound. On the other hand, the very long distances between the iron atoms, on which the magnetic orbitals of the ferracarborane anions are localized,¹⁴ preclude strong spin-coupling between the ions (shortest Fe-Fe distances (5), 9.88, (6), 9.28 Å). It is interesting that the compound $[\text{TTF}]^+[\text{Fe}(\text{C}_2\text{B}_9\text{H}_{11})_2]^-$ (2), in which the $[\text{TTF}]^+$ cations are also dimerized and the Fe-Fe distances are too long for significant orbital interaction between the Fe atoms (shortest Fe-Fe distance 6.34 Å), exhibits weak antiferromagnetic coupling between its anions ($\theta = -20$ K) (*vide supra*). This suggests that the thiophene groups may be involved in the mechanism of ferromagnetic coupling between the $[\text{Fe}(\text{C}_2\text{B}_9\text{H}_{11})_2]^-$ anions.

Electrical conductivity measurements on crystals of (5) and

(6) indicated that compound (5) is a semiconductor ($\sigma_{300\text{K}} = 2 \times 10^{-3}$ S cm⁻¹, activation energy = 0.22 eV) and compound (6) is an insulator ($\sigma_{290\text{K}} \leq 10^7$ S cm⁻¹)

2.3 ET Salts¹⁵

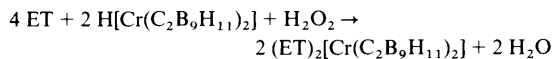
The TTF derivative bis(ethylenedithio)tetrathiafulvalene (ET) (see Figure 2) is another widely-used donor molecule for the synthesis of organic conductors, and has yielded the largest number of superconducting cation-radical salts.¹ The crystal structures of the ET salts usually consist of alternating layers of ET and anion molecules. The conducting behaviour of these salts are determined by their electronic and vibronic properties, which to a large extent are determined by the molecular packing and donor-donor and donor-anion interactions.¹ Thus, the size and shape of the anions are important factors governing the electrical properties of cation-radical salts of ET. In the β -(ET)₂X series of salts (X = linear triatomic monoanion), for example, whilst the isostructural $[\text{I}_3]^-$, $[\text{AuI}_2]^-$, and $[\text{IBr}_2]^-$ salts¹⁶⁻¹⁸ (type II in the nomenclature of Williams *et al.*)¹ are superconductors with transition temperatures (T_c 's) of 8, 5.0, and 2.8 K respectively, the salts of the smaller $[\text{Cl}_2]^-$ and $[\text{BrCl}]^-$ anions (type I or β' -phases) are semiconductors.^{1,19} This difference in behaviour has been attributed to the more anisotropic packing of ET molecules in the type I salts, which results in one-dimensional electronic band structures.²⁰ For the type II salts, the T_c 's increase with increasing anion size ($[\text{IBr}_2]^- < [\text{AuI}_2]^- < [\text{I}_3]^-$), although the T_c of 8 K for β -(ET)₂I₃ is attained with slight pressure (≈ 0.5 kbar) and shear.¹⁶

As part of our study of cation-radical salts of metallacarborane anions, the ET salts of the complexes *commo*-[3,3'-Cr(1,2-C₂B₉H₁₁)₂]⁻ and *commo*-[3,3'-Fe(1-(thiophene-2-yl)-1,2-C₂B₉H₁₀)₂]⁻ were synthesized. The use of monoanionic bis(dicarbollyl)metal complexes in this area is of interest because the complexes are rod-shaped and many of them are paramagnetic, making them good candidates for components of magnetic analogues of the existing β -phase ET salts. The study of such materials may contribute to the understanding of the relationship between magnetism and superconductivity.²¹ In particular, the chromacarborane complex chosen for study here combines high prolateness (length 12.8 Å, maximum cross-sectional radius 3.7 Å) and high spin ($S = 3/2$). Although its prolateness is close to that of the $[\text{Cl}_2]^-$ anion (length 8.7 Å, maximum cross-sectional radius 2.2 Å),^{1a} its length exceeds that of the $[\text{I}_3]^-$ anion (10.1 Å).^{1a} It is of interest to find out which of these parameters have a greater effect on the arrangement of ET molecules in the cation-radical salt. The thiophene-substituted ferracarborane $[\text{Fe}(1-(\text{thiophene-2-yl})-1,2-\text{C}_2\text{B}_9\text{H}_{10})_2]^-$ (4) ($S = 1/2$) is overall more discoidal in shape and hence is expected to favour a different packing motif of the ET molecules. Since weak ferromagnetic interactions have been observed in the tetrathiafulvalenium (TTF) salts of this anion ($\theta = 1.9$ and 0.5 K for $[\text{TTF}]_5[\text{Fe}(\text{C}_2\text{B}_9\text{H}_{10}\text{C}_4\text{H}_3\text{S})_2]_2$ and $[\text{TTF}]_2[\text{Fe}(\text{C}_2\text{B}_9\text{H}_{10}\text{C}_4\text{H}_3\text{S})_2]$ respectively (*vide supra*), it was hoped that the anion will favour ferromagnetic interactions in its ET salt as well.

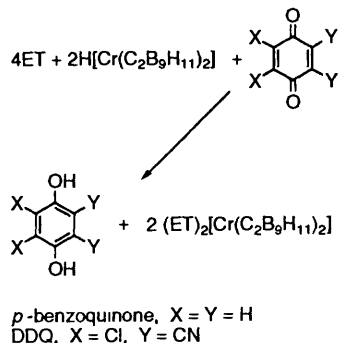
The majority of the reported ET salts were prepared by electrocrystallization. Chemical oxidation has only been employed in a few cases in which oxidizing precursors such as polyhalides or copper(II) halides were used.^{1,22} In most other cases, the lack of oxidizing precursors for the anions precluded synthesis by direct charge-transfer reactions. Although electrocrystallization is the best method for obtaining large single crystals of high quality, the conventional electrocrystallization apparatus suffers from the limitation that only a small amount of material can be produced each time. Furthermore, multiple phases are often formed at a single electrode and the relative yields of each phase are sensitive to subtle differences in crystallization conditions.¹ A reliable general method for the synthesis of ET salts *via* chemical oxidation is thus desirable.

On addition of H₂O₂ to a THF solution of ET and H[Cr(C₂B₉H₁₁)₂] at room temperature, the solution turned

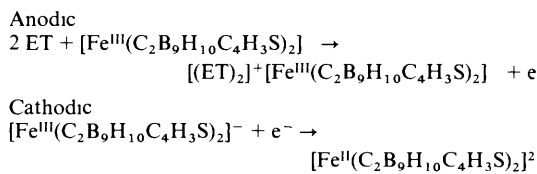
dark red-violet and shiny bronze needles of compound $(ET)_2[Cr(C_2B_9H_{11})_2]$ (10) (25% yield) slowly precipitated



The use of *p*-benzoquinone and 2,3-dichloro-5,6-dicyano-*p*-benzoquinone (DDQ) as oxidizing agents resulted in better yields of compound (10) (42 and 52% respectively)



The compound $(ET)_2[Fe(C_2B_9H_{10}C_4H_3S)_2]$ (11) was prepared by constant-current anodic oxidation of ET in the presence of $[NBu_4]^+[Fe(C_2B_9H_{10}C_4H_3S)_2]$ in 1,1,2-trichloroethane. The electrocrystallization was carried out under nitrogen in a two-chamber H-cell in which the anodic and cathodic compartments were separated by a fine-porosity glass frit. Black plate-like crystals of (11) were formed at the bottom of the anodic chamber after 2 to 4 weeks. The primary anodic and cathodic reactions are as follows



Layers of ET molecules and $[Cr(C_2B_9H_{11})_2]^-$ anions alternate along the *c*-direction in the crystals of (10), as shown in Figure 8. Each ET layer contains equivalent stacks of weakly-dimerized ET units which extend in the (010) direction. Short interstack S–S contacts (3.4–3.6 Å) link adjacent stacks. The intrastack S–S distances (> 3.7 Å) are much longer. All the ET molecules in the structure are parallel and are more-or-less coplanar along the interstack direction, as shown in Figure 9. Along the stack there are small longitudinal offsets between ET molecules within the dimers and pronounced sideways displacements, *i.e.* parallel to the short in-plane axes of the ET molecules, between dimers. The packing motif of ET molecules within the layer thus corresponds to that in the type I β' -(ET)₂X salts (X = $[ICl_2]^-$, $[BrICl]^-$), which feature a similar stepwise progression of ET dimers.²⁰ This indicates that the prolateness of the chromacarborane anion, rather than its length, has a greater effect on the packing of ET molecules. The ET molecules in (10) are more loosely packed than those in β' -(ET)₂(ICl₂) and β' -(ET)₂(BrICl). This is attributed to the large size of the $[Cr(C_2B_9H_{11})_2]^-$ anion.

Compound (11) has a unique structure because the anions form double layers with all the thiophene groups directed towards each other and away from the ET layers, as shown in Figure 10. This arrangement precludes the occurrence of S–S interactions between the ET molecules and the thiophene groups. There is no short S–S contact between thiophene groups. Both the DD and LL forms of the $[Fe(C_2B_9H_{10}C_4H_3S)_2]^-$ anion are present in the structure, the meso-isomer is not observed. The ET molecules are stacked along the (001) direction, and are engaged in weak pair-wise

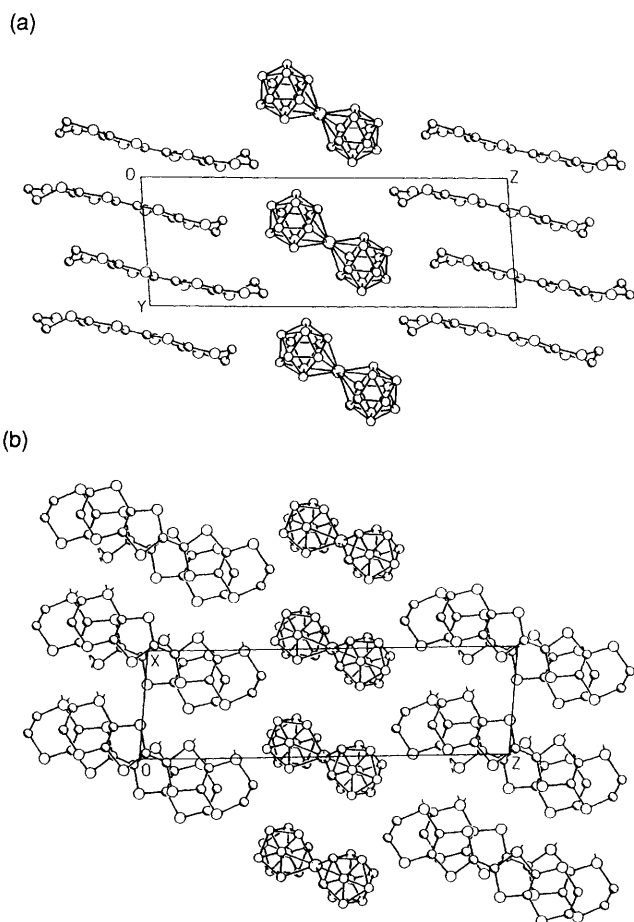


Figure 8 Packing diagrams of compound 10, showing the alternating layers of ET units and $[Cr(C_2B_9H_{11})_2]$ anions (a) view down the *a*-axis, (b) view down the *b*-axis (the dashed lines indicate S–S distances less than 3.7 Å)

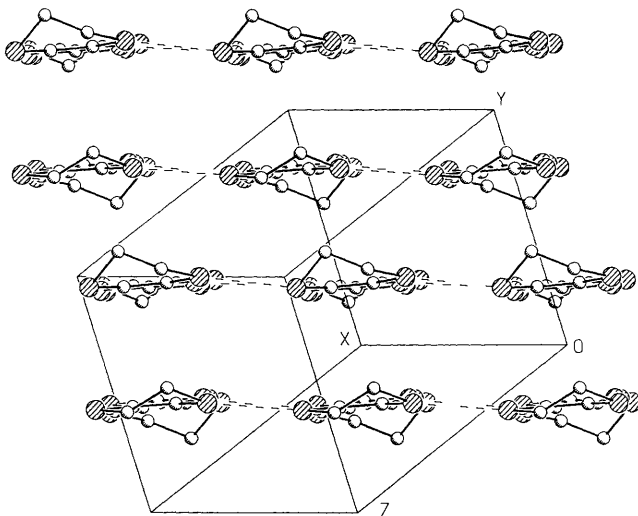


Figure 9 Diagram of a single layer of ET units in compound 10, viewed down the long axes of the ET units, showing the stepwise progression of ET dimers

interactions to form dimers. Adjacent stacks are displaced relative to each other along the stacking direction by approximately half the intrastack ET–ET distance, giving rise to a honeycomb network of interstack S–S interactions (Figure 11).

As in compound (10), the ET molecules in (11) are quite loosely packed. The packing in compound (11), however, is

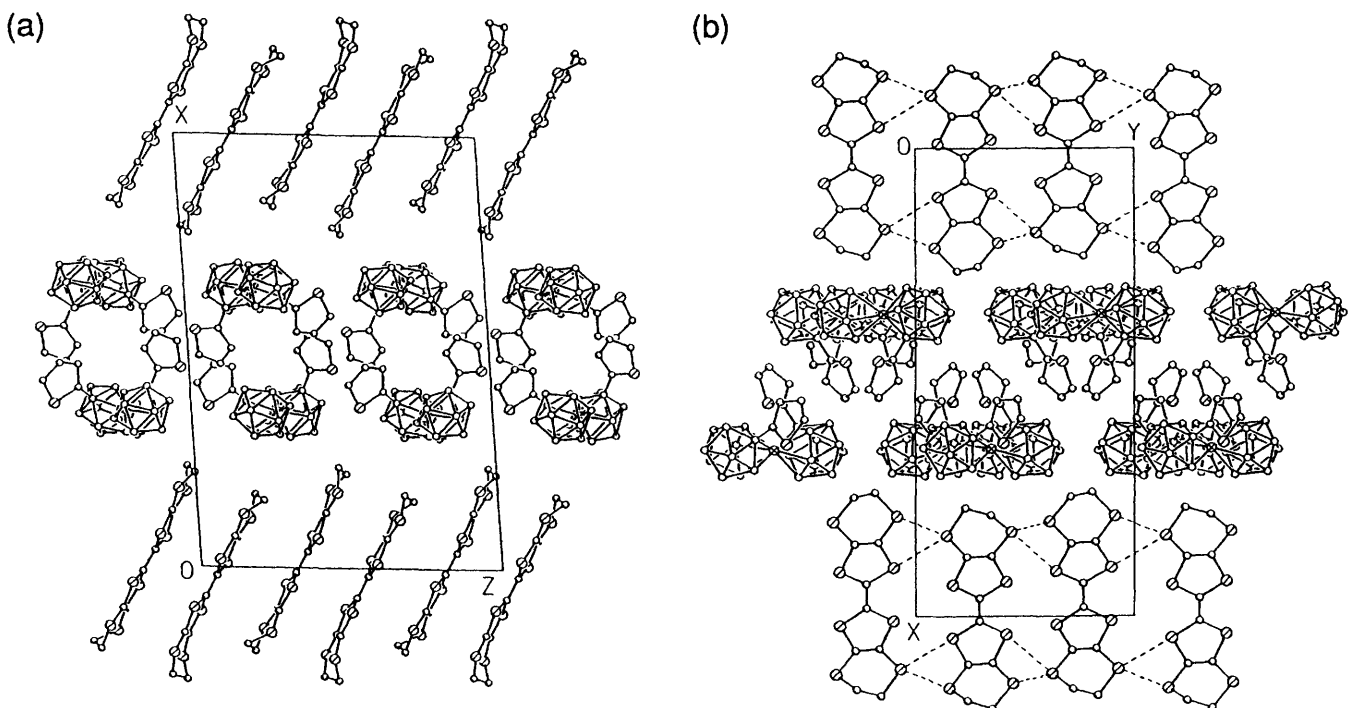


Figure 10 Packing diagrams of compound (11), showing the alternating ET single-layers and anion double-layers: (a) view down the *b*-axis, (b) view down the *c*-axis (the dashed lines indicate S···S distances shorter than 3.7 Å).

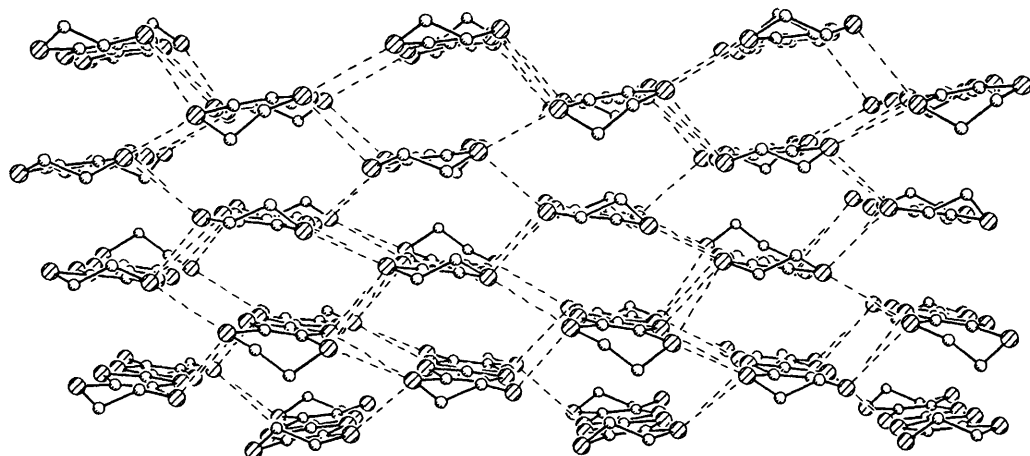


Figure 11 Illustration of the honeycomb network of intermolecular S···S interactions within a layer of ET units in compound (11).

more isotropic than that in compound (10). This is reflected in the narrower range of inter-ET centroid–centroid distances in (11).¹⁵

An intense, broad charge-transfer band at *ca.* 4000 cm^{−1} dominates the infrared (IR) spectra of both compounds (10) ($\tilde{\nu}_{\text{max}}$ 4400 cm^{−1}) and (11) ($\tilde{\nu}_{\text{max}}$ 4200 cm^{−1}). The presence of this electronic band (band A in the notation of Torrance *et al.*)²³ is consistent with the average charge of +0.5 on the ET molecules in compounds (10) and (11). It does not, however, indicate whether the valence electrons are equally delocalized over all the ET molecules ('mono-valence' configuration) or are localized on individual molecules, with the crystal lattice containing equal numbers of (ET)⁰ and (ET)⁺ molecules ('mixed-valence' configuration).

The optical spectra of both compounds (10) and (11) (as KBr pellets) exhibit a prominent band at *ca.* 10600 cm^{−1} (940 nm). This band, labelled 'B' by Torrance *et al.*, is attributed to charge-transfer transitions between singly-charged (ET)⁺ cations, *i.e.* [(ET)⁺, (ET)⁺] \rightarrow [(ET)⁰, (ET)²⁺].²³ The relatively high inten-

sity of band B in the spectra of (10) and (11) thus suggests the presence of (ET)⁺ molecules in compounds (10) and (11), and hence the adoption of mixed-valence configurations by compounds (10) and (11). A mixed-valence ET salt is expected to contain ET molecules with different geometries corresponding to their different charges. The fact that the ET molecules in compound (10) are all crystallographically equivalent can be explained by noting that the single-crystal X-ray diffraction experiment provides a time-averaged structure if the crystal structure being studied is fluxional on the time-scale of the experiment. Some charge-transfer salts of TTF and tetrathia-tetracene which are apparently mono-valent within the time-scale of X-ray crystallography²⁴ have been found to have mixed-valence configurations within the time-scale of X-ray photoelectron spectroscopy.²⁵

Compound (10) (as a compressed pellet) has a room-temperature electrical conductivity of *ca.* 2×10^{-3} S cm^{−1}. Variable-temperature resistance measurements (300–76 K) show that the conductivity of compound (10) is thermally activated. The

resistance data cannot, however, be fitted with the simple exponential law, $R = A \exp(E_a/kT)$, with constant activation energy E_a . The high- and low-temperature regions of the plot could be separately fitted with the exponential law to yield activation energies of 0.11 and 0.073 eV respectively.

The conductivity of crystals of compound (11) at room temperature is ca 0.5 S cm⁻¹. The resistance of the crystals exhibits complex temperature-dependence. Two main semiconducting regions are observed, both of which have a low activation energy of 0.046 eV. These regions differ in the mobility of the conduction electrons, as indicated by the difference in their fitted pre-exponential factor A . The gradient of the plot of $\ln R$ vs T^{-1} for compound (11) decreases gradually above 218 K and becomes nearly zero above ca 250 K. This suggests that compound (11) undergoes a gradual transition to a pseudo-metallic state above 218 K.

The relatively loose packing of the ET molecules in compounds (10) and (11) is expected to result in electronic bands with narrow bandwidths. Low-dimensional molecular conductors with narrow bandwidths are more unstable towards localization of conduction electrons and are therefore more likely to be non-metallic.²⁶ The semiconducting behaviours of compounds (10) and (11) are thus consistent with the nature of their molecular packing, especially for compound (10), which has a more anisotropic arrangement of ET molecules. This anisotropic character is expected to give rise to a one-dimensional band structure, thus making compound (10) more unstable towards a high-temperature metal-to-insulator transition.^{26,27}

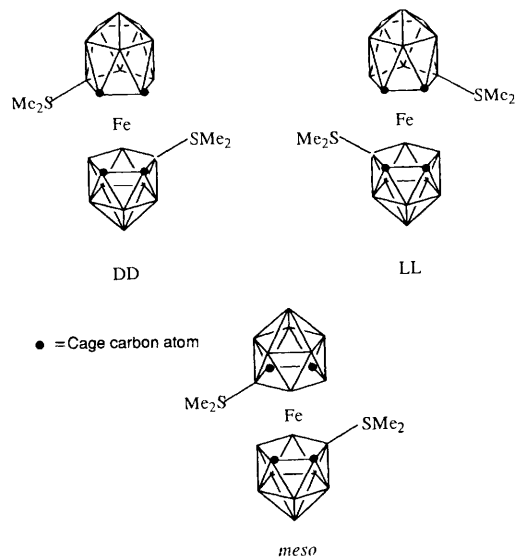
Between 25 and 300 K the corrected molar magnetic susceptibilities of compounds (10) and (11) follow the Curie-Weiss law, the θ values of -11 and $+16$ K respectively. The θ values indicate the presence of weak antiferromagnetic interactions in (10) and that of weak ferromagnetic interactions in (11). Since the shortest metal-metal (M-M) distances in compounds (10) and (11) are 6.6 and 9.2 Å respectively, no strong magnetic interactions between the spins in compounds (10) and (11) are expected.

2.4 DDQ Salts^{28,29}

As a complement to the study of molecular materials which contain anionic metallacboranes, the ferracarborane *common* $[3,3'-\text{Fe}\{4-(\text{Me}_2\text{S})-1,2-\text{C}_2\text{B}_9\text{H}_{10}\}_2]$ (12) and its charge-transfer salt with 2,3-dichloro-5,6-dicyano-*p*-benzoquinone (DDQ), $[3,3'-\text{Fe}\{4-(\text{Me}_2\text{S})-1,2-\text{C}_2\text{B}_9\text{H}_{10}\}_2]^+ [\text{DDQ}]^-$ (13) were synthesized.²⁸ Unusual metamagnetic and conducting charge-transfer salts of DDQ have previously been reported.³⁰ The charge-compensated ligand *nido*-[9-(Me₂S)-7,8-C₂B₉H₁₁] was chosen both for its ease of synthesis³¹ and because sulfur atoms have a propensity to engage in intermolecular bonding interactions,¹ which may enhance the electronic interactions between the cations and anions in the solid state.

Reaction of excess $\text{FeCl}_2(\text{thf})_2$ with a THF solution of $\text{Na}[9-(\text{Me}_2\text{S})-7,8-\text{C}_2\text{B}_9\text{H}_{10}]$ {freshly prepared by deprotonation of [9-(Me₂S)-7,8-C₂B₉H₁₁] (14) by NaH} at room temperature yielded a deep purple suspension from which (12) was isolated in 61% yield. Since the asymmetric ligand [9-(Me₂S)-7,8-C₂B₉H₁₀]⁻ is expected to be formed as a racemate, complex (12) should be produced as a mixture of *meso* (DL)-, *DD*-, and *LL*-isomers (Scheme 3). Interestingly, the isomers have very different solubility properties, and are very easily separated. Combination of *DD/LL*-(12) and DDQ in anhydrous dichloromethane solution yielded a black shiny crystalline precipitate of $[3,3'-\text{Fe}\{4-(\text{Me}_2\text{S})-1,2-\text{C}_2\text{B}_9\text{H}_{10}\}_2]^+ [\text{DDQ}]^-$ (13).

The molecular structures of the cation and anion in (13) are shown in Figure 12. This is the first example of a cationic metallacborane incorporating two dicarboride ligands to be crystallographically characterized. The $[3,3'-\text{Fe}\{4-(\text{Me}_2\text{S})-1,2-\text{C}_2\text{B}_9\text{H}_{10}\}_2]^+$ cation has non-crystallographic C_2 symmetry and adopts a staggered sandwich structure with the carbon atoms of the two dicarboride cages in a *cisoid* arrangement. The distance of the Fe atom from each C₂B₃ face (1.54 Å) is essentially the



Scheme 3 The stereoisomers of complex (12)

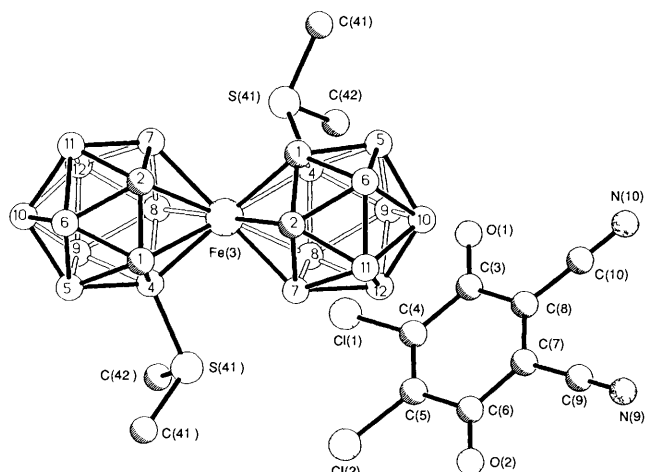


Figure 12 Molecular structures of the cation and anion in compound (13). The carbon atoms of the dicarboride cages are hatched

same as the corresponding distance in $[\text{TTF}]^+ [\text{Fe}(\text{C}_2\text{B}_9\text{H}_{11})_2]^-$ (2) (1.53 Å).

The cations and anions pack to form alternating layers in the crystal (Figure 13). Within the $[\text{DDQ}]^-$ layer, the anions form zig-zag chains linked via short intermolecular electrostatic N-Cl interactions [$\text{N}(9)-\text{Cl}(1a) = 3.21$ Å]. Similar electrostatic C≡N-Cl interactions have been observed in the crystal structures of several other chloro-cyano-compounds, *e.g.* substituted 1,2-dichloro-4,5-dicyanobenzenes and 4-chlorobenzonitriles,³² but not previously in DDQ and its compounds. The layer motif of the $[\text{DDQ}]^-$ anions observed here, which facilitates the formation of such 'molecular tapes', is also unprecedented. In the solid state, $[\text{DDQ}]^-$ anions usually form either segregated stacks (frequently with pair-wise interactions to form $([\text{DDQ}]^-)_2$ dimers)^{30b,33} or are interleaved with the cations to form mixed stacks.^{30a,34}

In addition to their mutual electrostatic attraction, the cation and anion layers are cross-linked by weak C-H-O hydrogen bonds between the oxygen atoms of the $[\text{DDQ}]^-$ anions and the hydrogen atoms attached to some of the carbon atoms of the dicarboride cages. The protonic character of the cage CH hydrogens of the $[3,3'-\text{Fe}\{4-(\text{Me}_2\text{S})-1,2-\text{C}_2\text{B}_9\text{H}_{10}\}_2]^+$ cation can be attributed to the presence of the charge-compensating Me₂S groups and the adjacent highly electron-attracting Fe^{III} atom. The cooperative effect of this hydrogen-bonding between the

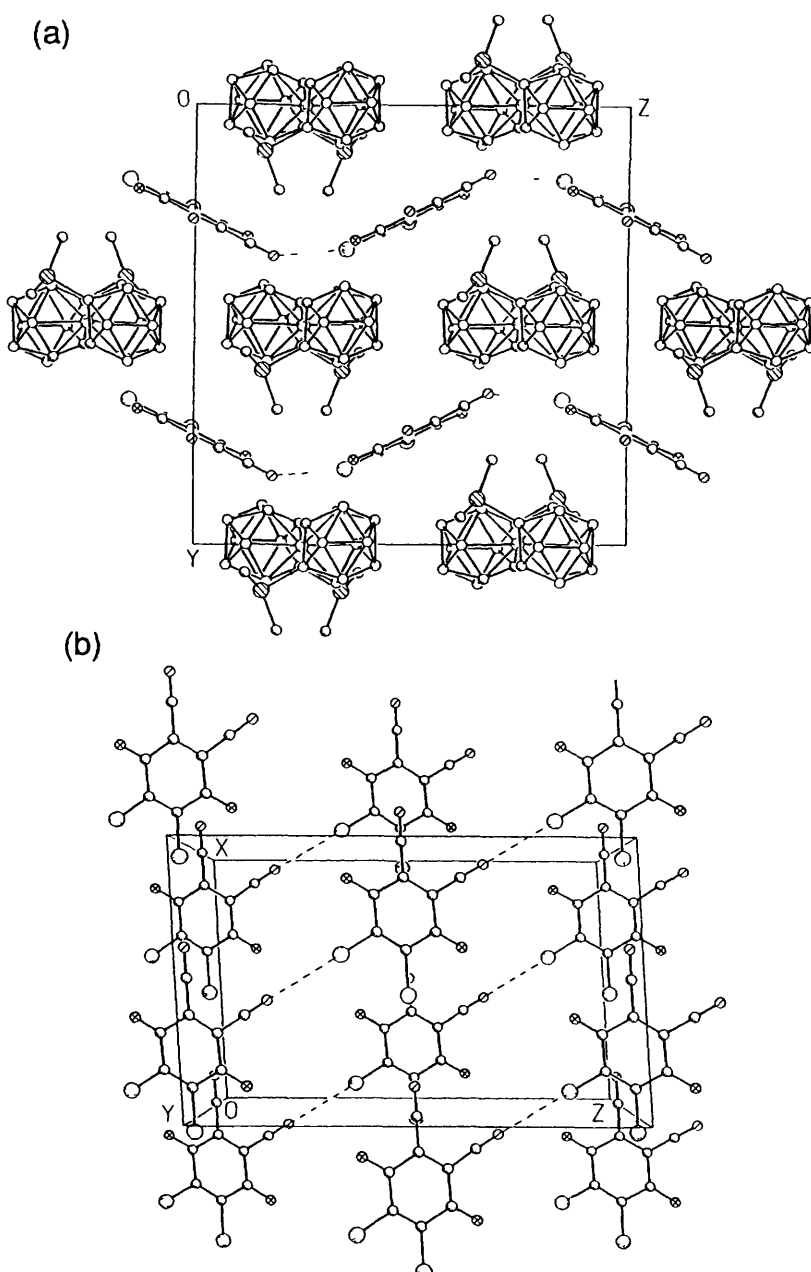


Figure 13 (a) Packing diagram of compound (13) showing the alternating layers of cations and anions (b) Diagram showing the packing of anions in (13)

cations and anions must play an important role in stabilizing the layered structure of compound (13)

Between 5 K and 270 K the corrected molar susceptibility of (13) follows the Curie-Weiss Law, with a θ value of -2.5 K , indicating that there is very weak interaction between the unpaired spins of the ions in (13). The unpaired spins on both the cations and anions contribute to the bulk magnetic susceptibility of the salt

No spin coupling between the metallacarbaborane cations in (13) is expected because there are no short inter-cationic contacts. Spin-spin interaction between the [DDQ]⁻ anions *via* the short C≡N—Cl contacts is also unlikely in the light of molecular orbital calculations by Miller and co-workers, which predict zero spin density on the Cl atoms of [DDQ]⁻ (reference 34b). Miller's calculations also indicate that within the [DDQ]⁻ radical anion, the highest spin densities reside on the quinoidal oxygen atoms. Thus, the overall lack of significant spin interaction in (13), despite the fact that two [DDQ]⁻ anions are hydrogen-bonded to each ferracarborane cation *via* the quinoi-

dal oxygen atoms, suggests that there is negligible delocalization of spin density from the Fe^{III} centre to the cage CH hydrogens in the [3,3'-Fe{4-(Me₂S)-1,2-C₂B₉H₁₀}]²⁺ cation

The room-temperature electrical conductivity of (13) (measured on a single crystal) is less than 10^{-8} S cm^{-1} . Thus, although the difference between the half-wave potentials of DD/LL-(12) and DDQ ($|\Delta E_{\frac{1}{2}}| = 0.04\text{ V}$) is small enough for the formation of a mixed-valence compound,^{30b} the failure to form DDQ stacks in the solid state results in the formation of an insulating solid

The mixed-sandwich complex *clos*-[3-(η^5 -Cp^{*}Fe){4-(Me₂S)-1,2-C₂B₉H₁₀}] (15) was also synthesized²⁹ in an attempt to study the effect of the Cp^{*} ligand on interionic magnetic interactions in metallacarbaborane analogues of $[(\text{Cp}^*)_2\text{Fe}]^+[\text{TCNE}]^-$. One of the proposed mechanisms for the ferromagnetism of the latter salt involves the delocalization of negative spin density onto the Cp^{*} rings of the $[(\text{Cp}^*)_2\text{Fe}]^+$ cation.⁴

The salt $[\text{Cp}^*\text{Fe}(\text{C}_2\text{B}_9\text{H}_{10}\text{SMe}_2)]^+[\text{DDQ}]^-$ (16) was obtained as a black microcrystalline precipitate in a direct

charge-transfer reaction of compound (15) with DDQ in dichloromethane. The $[\text{DDQ}]$ radical anions form isolated stacked dimers in the crystal structure of (16) CH_2Cl_2 , as shown in Figure 14. The short interplanar separation of 2.90 Å between the $[\text{DDQ}]$ units in the dimer is indicative of strong bonding interactions and spin-pairing between the two radical anions.³³ Each $[(\text{DDQ})_2]^2$ dimer is sandwiched between the Cp^* faces of two neighbouring $[\text{Cp}^*\text{Fe}(\text{C}_2\text{B}_9\text{H}_{10}\text{SMe}_2)]^+$ cations. The mean plane of the C_6 ring of each $[\text{DDQ}]$ anion makes an angle of $\approx 6^\circ$ to the Cp^* ring plane and the distance between the centroids of the two rings is 3.72 Å.

Compounds (16) is paramagnetic between 5 and 300 K, with a small Weiss constant, θ , of -0.9 K. The effective moment, μ_{eff} [$= \sqrt{(8\chi T)}$], of the compound is virtually independent of temperature in the above temperature range, and has an average value $\mu_{\text{av}} [= \sqrt{(8C)}]$ of $2.4 \mu_B$. This value, being close to that expected for a low-spin iron(III) complex ($2.3 \mu_B$), indicates that the organic radical anions in compound (16) do not contribute to the bulk magnetic susceptibility of the compound. This is consistent with the presence of $[(\text{DDQ})_2]^2$ dimers in the crystal structure of (16). It is thus not surprising that compound (16) does not exhibit any cooperative magnetic phenomenon.

Conductivity measurements were performed at room temperature on single crystals of compound (16), the conductivity of which was found to be less than $10^{-7} \text{ S cm}^{-1}$. The insulating nature of compound (16) is consistent with the presence of a strongly dimerized DDQ stack with negligible overlap between the $[(\text{DDQ})_2]^2$ dimers.

3 Summary

The research which is described above has demonstrated that it is possible to form a wide range of charge-transfer salts between

metallacarborane sandwich complexes and organic donors and acceptors. The stabilities of the metallacarborane sandwich compounds, especially with the metals in the +3 oxidation state, has meant that it is possible to synthesize comparable complexes with alternative *d*-electron configurations. The introduction of charge-compensating substituents onto the carborane cages has resulted in both anionic and cationic metallacarborane components in the resultant charge-transfer salts. The charge-transfer salts which have been made show many interesting features in the crystalline state. The DDQ tapers in $[\text{3,3'-Fe}\{4-(\text{Me}_2\text{S})-1,2-\text{C}_2\text{B}_9\text{H}_{10}\}_2]^+ [\text{DDQ}]$ (13) and the unusual sheet structure in the mixed valence TTF salt $[\text{TTF}]_5[\text{Fe}(\text{C}_2\text{B}_9\text{H}_{10}\text{C}_4\text{H}_3\text{S})_2]_2$ (5) are particularly novel. The intermolecular magnetic interactions in the charge-transfer salts have proved to be quite weak, presumably because the metal spin density is not effectively delocalized to the surface of the ions. Attempts to improve magnetic communication by introducing sulfur-containing substituents on the carborane ligands did not lead to significantly stronger magnetic interactions. Despite their large volumes the metallacarborane ions did not interfere with the formation of conducting TTF/ET arrays in many of the charge-transfer salts, which showed interesting variations in conductivity reflecting differences in the packing modes. The co-existence of magnetic ions and conducting organic arrays is a relatively rare occurrence, but is a common feature in these compounds.

Acknowledgements Support of this work by the EPSRC is acknowledged. Y-K Y thanks the Nanyang Technological University, Singapore, for a scholarship and D M P M thanks B P for a generous endowment.

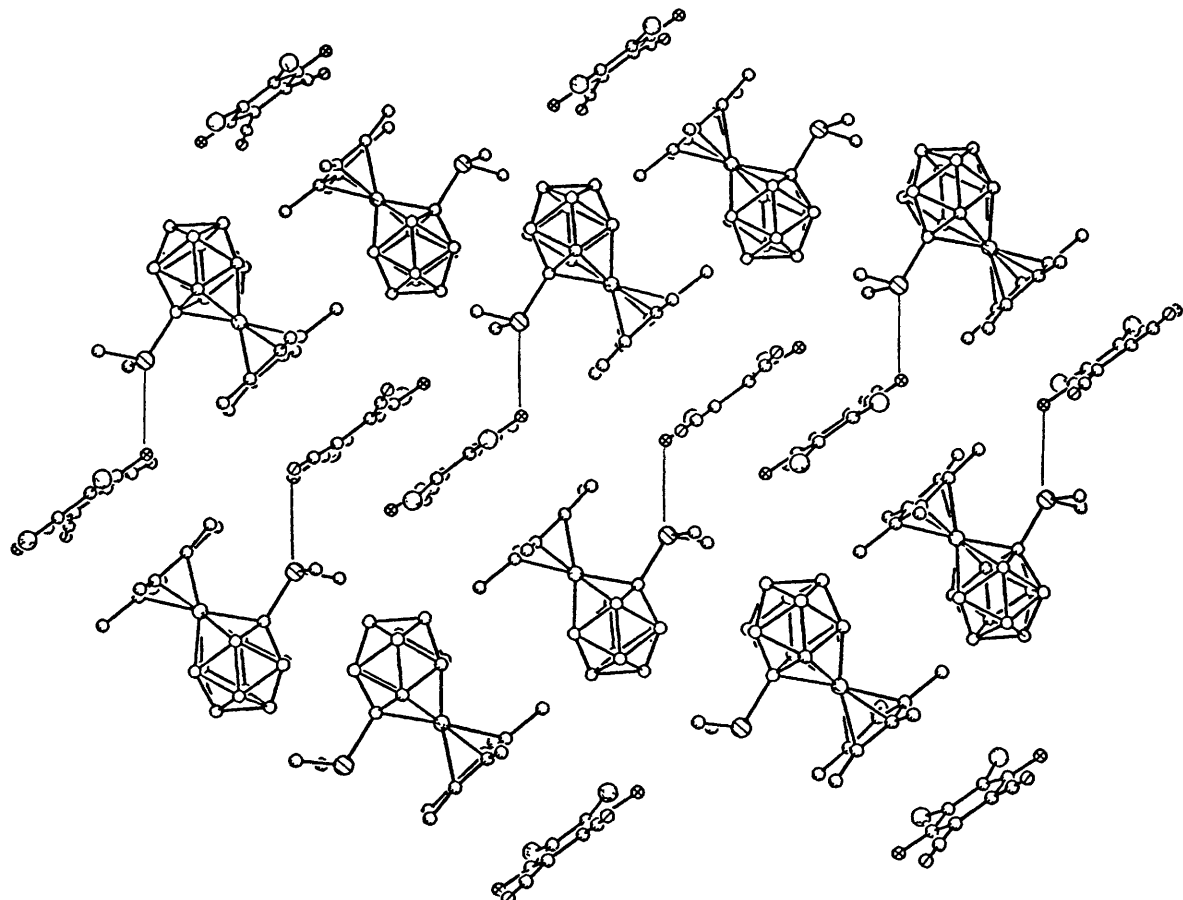


Figure 14 Diagram of the molecular packing in compound (16). The thin lines between the cations and anions indicate short S–O contacts.

4 References

- 1 (a) J M Williams, H H Wang, T J Emge, U Geiser, M A Beno, P C W Leung, K D Carlson, R J Thorn, A J Schultz, and M -H Whangbo, *Prog Inorg Chem*, 1987, **35**, 51 (b) J M Williams, J R Ferraro, R J Thorn, K D Carlson, U Geiser, H H Wang, A M Kini, and M -H Whangbo, 'Organic Superconductors (including Fullerenes) Synthesis, Structure, Properties and Theory', Prentice Hall, Englewood Cliffs, N J , 1992
- 2 J S Miller, A J Epstein, and W M Reiff, *Acc Chem Res*, 1988, **21**, 114
- 3 J S Miller, A J Epstein, and W M Reiff, *Chem Rev*, 1988, **88**, 201
- 4 (a) C Kollmar and O Kahn, *J Am Chem Soc*, 1991, **113**, 7987 (b) C Kollmar, M Couty, and O Kahn, *J Am Chem Soc*, 1991, **113**, 7994 (c) C Kollmar and O Kahn, *J Chem Phys*, 1992, **96**, 2988
- 5 (a) H W Ruhle and M F Hawthorne, *Inorg Chem*, 1968, **7**, 2279 (b) M F Hawthorne, D C Young, T D Andrews, D V Howe, R L Pilling, A D Pitts, M Reintjes, L F Warren, Jr , and P A Wegner, *J Am Chem Soc*, 1968, **90**, 879 (c) L F Warren, Jr and M F Hawthorne, *J Am Chem Soc*, 1970, **92**, 1157 (d) C G Salentine and M F Hawthorne, *Inorg Chem*, 1976, **15**, 2872 (e) L F Warren, Jr and M F Hawthorne, *J Am Chem Soc*, 1968, **90**, 4823
- 6 R N Grimes, in 'Comprehensive Organometallic Chemistry', ed G Wilkinson, F G A Stone, and E W Abel, Pergamon, Oxford, 1982, Volume 1, Chapter 5 5, p 459
- 7 J M Forward, D M P Mingos, T E Muller, D J Williams, and Y -K Yan, *J Organomet Chem*, 1994, **467**, 207
- 8 F Wudl, *J Am Chem Soc*, 1975, **97**, 1962
- 9 (a) Y -K Yan, D M P Mingos, M Kurmoo, W -S Li, I J Scowen, M McPartlin, A T Coomber, and R H Friend, *J Chem Soc Chem Commun*, 1995, 997 (b) Y -K Yan, D M P Mingos, M Kurmoo, W -S Li, I J Scowen, M McPartlin, A T Coomber, and R H Friend, *J Chem Soc Dalton Trans* . in press
- 10 C Bellitto, M Bonamico, V Fares, P Imperatori, and S Patrizio, *J Chem Soc Dalton Trans*, 1989, 719
- 11 J S Kasper, L V Interrante, and C A Secaur, *J Am Chem Soc*, 1975, **97**, 890
- 12 K Kikuchi, K Yakushi, H Kuroda, I Ikemoto, K Kobayashi, M Honda, C Katayama, and J Tanaka, *Chem Lett*, 1985, 419
- 13 E Hernandez, M Mas, E Molins, C Rovira, and J Veciana, *Angew Chem Int Ed Engl*, 1993, **32**, 882
- 14 D M P Mingos, in 'Comprehensive Organometallic Chemistry', ed G Wilkinson, F G A Stone, and E W Abel, Pergamon, Oxford, 1982 Volume 3, Chapter 19, pp 32—33
- 15 Y -K Yan, D M P Mingos, D J Williams, and M Kurmoo, *J Chem Soc Dalton Trans* , in press
- 16 (a) K Murata, M Tokumoto, H Anzai, H Bando, G Saito, K Kajimura, and T Ishiguro, *J Phys Soc Jpn*, 1985, **54**, 2084 (b) J E Schirber, L J Azevedo, J F Kwak, E L Venturini, P C W Leung, M A Beno, H H Wang, and J M Williams, *Phys Rev B*, 1986, **33**, 1987 (c) J E Schirber, J F Kwak, M A Beno, H H Wang, and J M Williams, *Physica B*, 1986, **143**, 343
- 17 H H Wang, M A Beno, U Geiser, M A Firestone, K S Webb, L Nuñez, G W Crabtree, K D Carlson, J M Williams, L J Azevedo, J F Kwak, and J E Schirber, *Inorg Chem*, 1985, **24**, 2465
- 18 J M Williams, H H Wang, M A Beno, T J Emge, L M Sowa, P T Copps, F Behroozi, L N Hall, K D Carlson, and G W Crabtree, *Inorg Chem*, 1984, **23**, 3839
- 19 M Tokumoto, H Anzai, T Ishiguro, G Saito, H Kobayashi, R Kato, and A Kobayashi, *Synth Met*, 1987, **19**, 215
- 20 T J Emge, H H Wang, P C W Leung, P R Rust, J D Cook, P L Jackson, K D Carlson, J M Williams, M -H Whangbo, E L Venturini, J E Schirber, L J Azevedo, and J R Ferraro, *J Am Chem Soc*, 1986, **108**, 695
- 21 P Day, *Chem Soc Rev*, 1993, 51
- 22 M Kurmoo, D R Talham, P Day, J A K Howard, A M Stringer, D S Obertelli and R H Friend, *Synth Met*, 1988, **22**, 415
- 23 J B Torrance, B A Scott, B Welber, F B Kaufman, and P E Seiden, *Phys Rev B*, 1979, **19**, 730
- 24 (a) T J Kistenmacher, T E Phillips, and D O Cowan, *Acta Crystallogr Sect B*, 1974, **30**, 763 (b) B A Scott, S J La Placa, J B Torrance, B D Silverman, and B Welber, *J Am Chem Soc*, 1977, **99**, 6631 (c) D L Smith and H R Luss, *Acta Crystallogr Sect B*, 1977, **33**, 1744
- 25 I Ikemoto, M Yamada, T Sugano, and H Kuroda, *Bull Chem Soc Jpn*, 1980, **53**, 1871
- 26 S S Shaik and M -H Whangbo, *Inorg Chem*, 1986, **25**, 1201
- 27 R E Peierls, 'Quantum Theory of Solids', Oxford University Press, London, 1955, p 108
- 28 Y -K Yan, D M P Mingos, T E Muller, D J Williams, and M Kurmoo, *J Chem Soc Dalton Trans* , 1994, 1735
- 29 Y -K Yan, D M P Mingos, T E Muller, D J Williams, and M Kurmoo, *J Chem Soc Dalton Trans* , in press
- 30 (a) J S Miller, R S McLean, C Vazquez, G T Yee, K S Narayan, and A J Epstein, *J Mater Chem*, 1991, **1**, 479 (b) J J Mayerle and J B Torrance, *Bull Chem Soc Jpn*, 1981, **54**, 3170
- 31 J Plesek, Z Janousek, and S Hermanek, *Inorg Synth* , 1983, **22**, 239
- 32 (a) G R Desiraju and R L Harlow, *J Am Chem Soc* , 1989, **111**, 6757 (b) D S Reddy, K Panneerselvam, T Pilati, and G R Desiraju, *J Chem Soc Chem Commun* , 1993, 661
- 33 (a) L Pasimeni, M Brustolon, P L Zanonato, and C Corvaja, *Chem Phys*, 1980, **51**, 381 (b) A Marzotto, D A Clemente, and L Pasimeni, *J Crystallogr Spectrosc Res* , 1988, **18**, 545
- 34 (a) E Gebert, A H Reis, Jr , J S Miller, H Rommelmann, and A J Epstein, *J Am Chem Soc* , 1982, **104**, 4403 (b) J S Miller, P J Krusic, D A Dixon, W M Reiff, J H Zhang, E C Anderson, and A J Epstein, *J Am Chem Soc* , 1986, **108**, 4459